







Determination of the Metallic Coating Properties Obtained by Thermal Spraying and Analysis of its Influence on the Heat Transfer Efficiency in the Thermoelectric Power Plant Boiler Tubes

Pamella Kessler de Campos¹ , Bruno Reis Cardoso² , Heloísa Cunha Furtado² , Vitor Santos Ramos³ , André Rocha Pimenta⁴ ,
Marília Garcia Diniz¹ 

¹ Universidade do Estado do Rio de Janeiro – UERJ, Rio de Janeiro, RJ, Brasil.

² Centro de Pesquisas de Energia Elétrica – CEPTEL, Rio de Janeiro, RJ, Brasil.

³ Universidade Federal do Rio de Janeiro – UFRJ, Instituto de Macromoléculas Professora Eloisa Mano – IMA, Rio de Janeiro, RJ, Brasil.

⁴ Instituto Federal do Rio de Janeiro – IFRJ, Rio de Janeiro, RJ, Brasil.

How to cite: Campos PK, Cardoso BR, Furtado HC, Ramos VS, Pimenta AR, Diniz MG. Determination of the metallic coating properties obtained by thermal spraying and analysis of its influence on the heat transfer efficiency in the thermoelectric power plant boiler tubes. *Soldagem & Inspeção*. 2022;27: e2716. <https://doi.org/10.1590/0104-9224/SI27.16>

Abstract: Mineral coal is a fuel that can be used by thermoelectric plants to generate electricity, however, the solid residues of its combustion, so-called ash, cause erosion and corrosion in the internal components of boilers that operate at high temperatures, causing failures in the system. This study proposes a metallic coating based on Fe-Cr-Si, obtained using the electric arc thermal spray technique as an alternative for protecting the most affected parts of boiler tubes by the ash impact. Optical microscopy (OM), scanning electron microscopy (SEM), semi-quantitative chemical analysis by Energy Dispersive Spectroscopy (EDS), X-ray diffraction (XRD), roughness measurements, pull-off adhesion tests were used. Thermal diffusivity measurements and mathematical modelling were elaborated to evaluate the thermal exchange efficiency impact of the coating in thermoelectric plant boiler tubes. The results showed that the chemical components of the sprayed wire were well incorporated into a coating with a hardness of 730.54 ± 164.28 HV, approximately three times greater than the hardness of boiler pipes and only 11% less than the hardness of ash. XRD identified the presence of crystalline phases in the coating and adhesion tests showed that the failures were cohesive without substrate exposure. The presence of the coating reduced heat exchange of approximately 0.64% / tube length. These results showed that the proposed coating, which has a lower cost compared to others, be a promising solution to avoid unscheduled shutdowns in thermoelectric boilers.

Key-words: Metallic coating; Thermal spray; Heat transfer; Thermoelectric power plant; Coal fired boiler plant.

1. Introduction

When pulverized coal is burned to obtain energy in thermoelectric power plants, highly hard residues containing aluminum, silicon and iron oxides, so-called ash, are generated [1,2].

The ash is responsible for causing erosion and corrosion in the internal boiler components and has a hardness around 825 HV, depending on its composition [3,4]. The impact severity of these particles can cause on the internal boiler components varies from component to component, with the water wall tubes being one of the most affected elements of the system. These particles are projected onto the water wall and, eventually, over time, cause the surface to deteriorate, causing the erosion process associated or not with corrosion, which reduce the tube thickness, causing its rupture [5].

In this sense, the coating technology presents itself as an alternative to provide the longevity of these tubes and avoid unscheduled stops, which cause damage. Studies carried out identified that coatings based on Ni, WC, Al, or Cr are the most used to coat tubes in boiler systems [6,7]. One of the deposition techniques for metallic coatings widely used is thermal spraying (TS) by electric arc (ASP - Arc Spray Process) due to its low application cost, high deposition rate, ease field reproduction, wire variety that can be used, good coating thickness control and efficiency in its performance [8].

This study metallurgically characterized and model the thermal exchange behavior of a metallic coating obtained using ASP, aiming at its application in thermoelectric plants boiler tubes, to minimize the damage caused by the ash particle impact and consequently increase the longevity of the internal components and avoid unscheduled stops.

Received: 21 Mar., 2022. Accepted: 27 June, 2022.

E-mails: pamella.kessler@gmail.com, brunorc@cepel.br, heloisa@cepel.br, vramos00@gmail.com, andre.pimenta@ifrj.edu.br, mgarciadiniz@gmail.com



This is an Open Access article distributed under the terms of the [Creative Commons Attribution license](https://creativecommons.org/licenses/by-nc/4.0/), which permits unrestricted use, distribution, and reproduction in any medium, provided the original work is properly cited.

2. Materials and Methods

The analyzed coating was applied on a substrate with a chemical composition like that of the tubes used in boilers of thermoelectric power plants and which are classified ASTM A 178 - grade A [9]. The substrate was subjected to Sa 2½ [10] dry abrasive blast cleaning and surface preparation using G16 / 20 mesh (1.19 / 0.84 mm) angled alumina. After sandblasting, with the aid of an analog roughness meter model Ry-5, 100 measurements of substrate surface roughness were performed, with an average value of $116.8 \pm 20.33 \mu\text{m}$.

The wire chemical composition used to spray onto the substrate surface using the TS technique to form the coating is as shown in Table 1.

The wire used in this research was commercial and the diameter of the wire used was 1.6 mm. The wire commercial name was not provided by the partner company that carried out the spraying process. This engineering company has expertise in this field of application and established the spray parameters used here based on their experience with thermal spraying of metallic coatings like the one studied here. The deposition parameters used were suggested for obtaining a coated layer without great porosity and with homogeneity in the adhesion force on the substrate surface. The spray was performed manually at an angle between the gun and the plate of 90 degrees using a specific equipment. The spray parameters are shown in Table 2.

Table 1. Chemical composition of the wire.

Elements (% Weight)	Silicon	Chromium	Manganese	Boron	Iron
Wire	1.6	29	1.65	3.75	Balance

Table 2. Electric arc sprayed parameters.

Voltage (V)	30
Current (A)	100
Atomizing air pressure (kPa)	480
Projection distance (mm)	100
Deposition rate (kg/h)	5

To fabricate the specimens, three substrate plates measuring 150 x 100 mm were coated and 17 samples were taken from them for the characterization techniques used in this study: 1 for coating roughness measurements, 1 for optical microscopy (OM) and macrographs, 1 for Vickers microhardness measurements (HV), 1 for scanning electron microscopy (SEM) and semi-quantitative chemical analysis by Energy Dispersive Spectroscopy (EDS), 8 for pull-off adhesion assays, 4 for thermal diffusivity measurements and 1 for X-ray diffraction (XRD). The coating was deposited on a flat surface substrate (and not on tubes) to allow compliance with the standards for adhesion tests, obtaining thermal diffusivity measurements and the DR-X technique, since the lack of flatness of samples would impair the use of such techniques.

The roughness of the sprayed coating was obtained using a digital rugosimeter with a measuring range of 0 – 1000 μm and a resolution of 1 μm . To calculate the coating average roughness (Ra), 100 measurements were considered.

Samples for OM, microhardness, analysis by SEM, EDS and XRD were cut with the aid of an metallographic cutter, model Arocor 80. The samples for MO, microhardness, analysis by SEM, were embedded in bakelite and sanded manually with water sandpaper in the granulometric sequence of 220, 440, 600, 800, and 1200 mesh. After sanding, the samples were submitted to polishing with diamond paste in the granulometric sequence of 6 μm , 3 μm , and 1 μm .

OM images were obtained using an optical microscope model Axio Imager M1m, with a digital image acquisition system and controlled by the Carl Zeiss AxioVision 40 V 4.8.2.0 software.

Macrographic aspects were obtained using a stereoscope model SZX7.

SEM analyses used a Schottky Field Emission Gun (FEG-MEV) model MIRA operating at 10 keV and equipped with an EDS detector with a 30 mm² Si₃N₄ window and a resolution lower than 129 eV in Mn K α . Analysis were also performed using TM3000 equipment, with a EDS detector system operating at 15 keV, low vacuum, working distance of 7.7 mm and scanning at intervals of 10 minutes each. The results obtained were analyzed by the program Quantax and PYMAC.

Vickers microhardness (HV) measurements were performed on the substrate, at the interface between the substrate and coating and on the coating itself. Three measurement grids were performed with 18 indentation points each, in each region of interest. The spacing between measurements was 100 μm . A microhardness tester model MV-1000A was used, load of 100 grams (0.9807 N), time of 15 seconds of load application and according to the ABNT NBR NM ISO 6507-1 standard [11].

Measurements of the thermal diffusivity of the coating / substrate system were performed according to the Standard Test Method for Thermal Diffusivity (Flash Method) according to ASTM E1461 [12] and a LFA 447 model equipment was used. The

specimens with dimensions of 12.7 x 12.7 mm and thicknesses between 1 and 2 mm were cleaned by means of ultrasound in an analytically pure acetone bath for 10 minutes. A thin layer of Farnell type Graphit 33 graphite was placed on them. The samples thermal diffusivity was measured in four different temperatures (25°C, 50°C, 100°C and 200°C), then an average value was calculated.

Heat transfer analysis in boiler tubes has been widely studied by several authors [13,14]. In this study, to analyze the impact of the coating on the efficiency of heat transfer in the boiler water wall, a one-dimensional model was developed considering the steady-state radial heat conduction through cylindrical walls and the thermal conductivity of the coating [15].

The thermal conductivity (k) can be expressed from the thermal diffusivity (α), the density (ρ) and the volumetric heat capacity of the material (C_p), according to Equation 1. The coating density was provided by the manufacturer and for C_p , the average value of this property for iron-based alloys was considered.

$$k = \alpha \rho C_p \quad (1)$$

Considering the general expression of heat flux and the Fourier equation for radial heat conduction, we have the Equation 2:

$$\frac{1}{r} \frac{d}{dr} \left(kr \frac{dT}{dr} \right) = 0 \rightarrow q_r = -kA \frac{dT}{dr} = -k(2\pi rL) \frac{dT}{dr} \quad (2)$$

where $A=2\pi rL$ is the area normal to the heat transfer and q_r is the heat transfer rate in the radial direction, r is the inner radius, L is the longitudinal length transverse to the heat flow and T is the temperature.

For a cylindrical shell subjected to a temperature difference between the inner surface and the outer surface of $T_1 - T_2$, where the inner surface temperature is constant and equal to T_1 , while the outer surface temperature remains constant and equal to T_2 , heat transfer by conduction is in the steady state, which is the case with boilers in thermoelectric plants.

The solution of Equation 2 for generic boundary conditions, that is, for temperature T_{s1} at radial position r_1 and temperature T_{s2} at radial position r_2 :

$$T(r_1) = T_{s,1} \rightarrow T_{s,1} = C_1 \ln r_1 + C_2 \quad (3)$$

$$T(r_2) = T_{s,2} \rightarrow T_{s,2} = C_1 \ln r_2 + C_2 \quad (4)$$

Solving C1 e C2, we have:

$$T(r) = \frac{T_{s,1} - T_{s,2}}{\ln\left(\frac{r_1}{r_2}\right)} \ln\left(\frac{r}{r_2}\right) + T_{s,2} \quad (5)$$

Thus, thermal resistance (R) of Equation 5 will have the form:

$$R_{t,cond} = \frac{\ln\left(\frac{r_2}{r_1}\right)}{2\pi Lk} \quad (6)$$

Figure 1 schematizes the cross-section formed by the system present in the boiler tubes, which is formed by thermal resistances in series of the convective film of water inside the tubes, the wall of the tube, the external coating and the external convective film of gas. Neglecting the contact resistances, the heat transfer rate by conduction ($q_r - \text{KW}$) in the system formed by thermal resistances in series will be given by the Equation 7:

$$q_r = \frac{T_{\infty,1} - T_{\infty,2}}{\frac{1}{2\pi r_1 L h_1} + \frac{\ln\left(\frac{r_2}{r_1}\right)}{2\pi k_A L} + \frac{\ln\left(\frac{r_3}{r_2}\right)}{2\pi k_B L}} = \frac{T_{\infty,1} - T_{\infty,2}}{R_{tot}} \quad (7)$$

Where:

h_1 = average value of the convection heat transfer coefficient for the environment 1 – W/(m²K).

h_3 = average value of the convection heat transfer coefficient for the environment 3 – W/(m²K).

K_A = thermal conductivity for material A – steel pipe – W/(mK).

K_B = thermal conductivity for material B – coating – W/(mK).

R_{TOT} = total system resistance – W/(m²K).

The conduction heat transfer rate can also be expressed in terms of the global heat transfer coefficient ($U - \text{W}/(\text{m}^2\text{K})$) by the Equation 8 [15]:

$$q_r = \frac{T_{\infty,1} - T_{\infty,2}}{\frac{1}{2\pi r_1 L h_1} + \frac{\ln(\frac{r_2}{r_1})}{2\pi k_A L} + \frac{\ln(\frac{r_3}{r_2})}{2\pi k_B L}} = \frac{T_{\infty,1} - T_{\infty,2}}{R_{tot}} = UA (T_{\infty,1} - T_{\infty,2}) \quad (8)$$

If the overall heat transfer coefficient (U) is defined in terms of the inner surface area, $A_1=2\pi r_1 L$, then we have Equation 9:

$$U = \frac{1}{\frac{1}{h_1} + \frac{r_1}{k_A} \ln \frac{r_2}{r_1} + \frac{r_1}{k_B} \ln \frac{r_3}{r_2} + \frac{1}{h_3}} \quad (9)$$

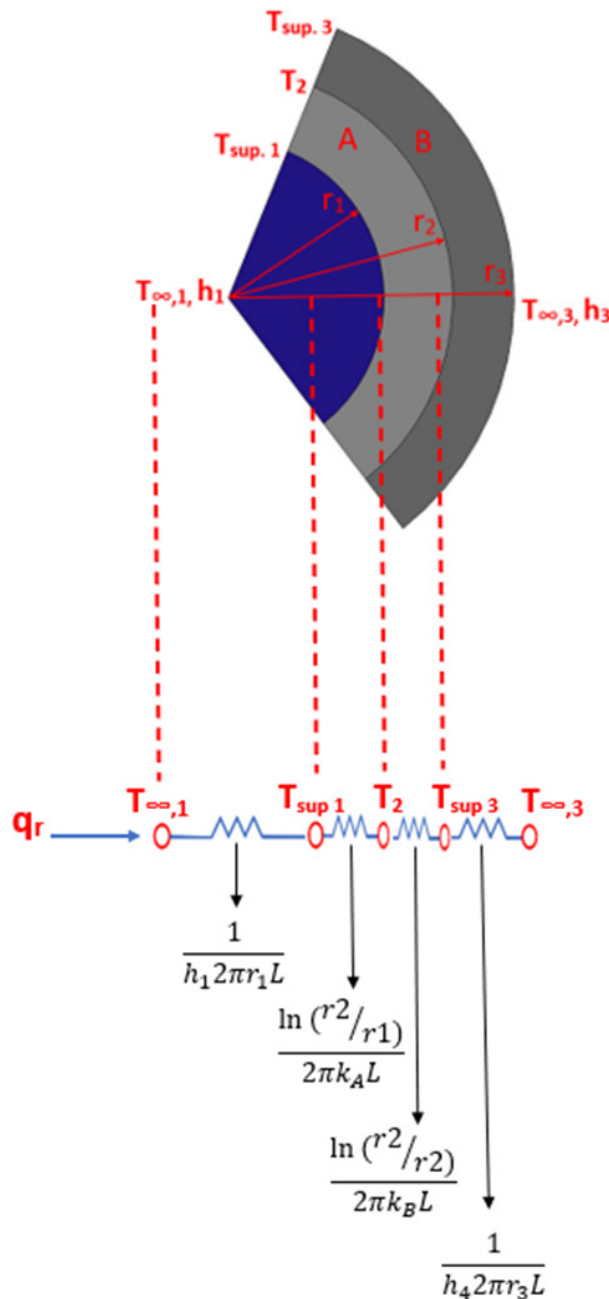


Figure 1. Schematic of the temperature distribution in a cylindrical wall system composed of thermal resistances in series. Image adapted from [15].

To predict the effect of coating application on the heat exchange between the hot gases generated by the burner and water flowing inside the tubes, the heat transfer rate efficiency (η) was calculated (Equations 10 - 12). The calculations were performed for the following considerations:

- a) Without the presence of the coating (not isolated);
- b) Considering the presence of the coating (isolated), the thermal diffusivity was obtained experimentally.

$$\eta = \frac{q_{isolated}}{q_{non-isolated}} = \frac{UA\Delta T_{isolated}}{UA\Delta T_{non\ isolated}} \quad (10)$$

$$\Delta T_{isolated} = \Delta T_{non\ isolated} \quad (11)$$

$$\eta = \frac{q_{isolated}}{q_{non\ isolated}} = \frac{UA_{isolated}}{UA_{non\ isolated}} \quad (12)$$

The heat transfer area for all cases was defined by $A=2\pi rL$, varying as a function of the internal and external radii (0.0225 m and 0.0295 m respectively) and the useful length of the tube (1 m). Average values were adopted for the convection heat transfer coefficients for condensation / vaporization 51250 W/m²K and 137.5 W/m²K respectively [15] and a conductivity coefficient for the boiler tubes of 81 W/m °K.

The adhesion test that evaluated the mechanical/metallurgical interaction of the coating with the substrate was performed according to the Cohesion Strength of Coatings by Thermal Spray of the ASTM C633 [16] standard. Eight samples with a diameter of 20 mm were tested, arranged and fixed using 3M Scotch Weld DP-460 adhesive. The spools were arranged on two plates measuring 150 x 100 mm each, coupled to a universal testing machine, EMIC model DL-30000, and pulled by a load of 50 kN at a speed of 1 mm/minute.

Substrate and coating samples were analyzed for present phases by X-ray diffraction (XRD) using a Rigaku Ultima IV diffractometer with a 285 mm radius goniometer. The measurements used a tube with a copper anode, incidence slit of 2/3, 10 mm mask, 0.6 mm diffracted beam slit, power 40 keV and 40 mA, Bragg Brentano scan of 2θ (5 - 100) °, 0.05° step, 10 - seconds time per step.

3. Results and Discussion

Figures 2 and 3 present the aspect of the cross-section of the substrate/coating system in the OM, where the coating presented superimposed metallic layers of flattened lamellae, typically associated with metallic coatings obtained by ASP. A series of heterogeneities is inherent in the thermal spraying process. Discontinuities in the coating microstructure (pores, oxides, and cracks) obtained by thermal spraying are common and their quantity and distribution can considerably limit their useful life and performance in service. The presence of pores and cracks in the coating can generate permeability with harmful effects for the substrate, such as loss of adhesion at the substrate-coating interface, failure to protect against corrosion and decrease in the coating thermal conductivity. The presence of oxide networks, in turn, can reduce the adhesion between lamellae and substantially increase the coating hardness, making it brittle. Controlling the parameters of thermal spray coating processes mitigates and minimize the presence of these defects.

Some percentage of porosity in metallic coatings is part of the characteristic of materials sprayed using the electric arc process, and it is recommended that this porosity be as low as possible due to the damaging effect on the coating cohesion. Furthermore, when these void regions form in an interconnected manner, the presence of direct paths from the ambient atmosphere to the substrate can become preferential sites for corrosion processes Lacerda et al. [17]. Some typical defects (such as cracks and pores) can be observed in Figures 2 and 3. Similar aspects were found by Vaz et al. [18], Šulcová et al. [19], Lacerda et al. [17], Gomes [3], Zhang et al. [20], Azarmi and Sevostianov [21] for coatings obtained using the same technique, some of them with a wire chemical composition similar to that used in this study. Cracks and pores appeared as dark regions in the OM images, the particles unfused during spraying as light and spherical regions.

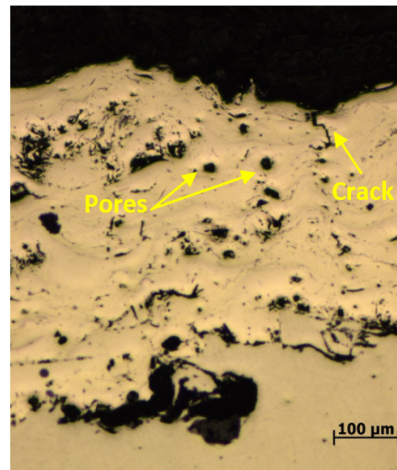


Figure 2. Microstructural aspect of the metallic coating with the presence of defects typically associated with the electric arc spray method.



Figure 3. Cross-section of the substrate/coating system.

The coating had a thickness of $337.40 \pm 52.89 \mu\text{m}$ and an average roughness (Ra) of $247.84 \pm 63.46 \mu\text{m}$. In the metallic coating obtained by ASP proposed by Kant et al. [20], the Ra found was $2.986 \mu\text{m}$. Arif et al. [22] obtained $Ra = 6 \mu\text{m}$. Cossenza [23] obtained $Ra = 51 \mu\text{m}$ for metallic coating and using electric arc spray parameters similar to those used in this study.

The deposited thickness and surface roughness are values that are strongly dependent on the TS parameters used and affect not only the effectiveness of the system's heat exchanges, but also the resistance to wear by the impact of particles in the boiler environment [24,25]. TS parameters influence the surface finish and its morphological appearance [22]. Erodent particles tend to act more aggressively on surfaces with high roughness, thus reducing their useful life. One of the possible reasons for the high roughness found here have been the spraying distance adopted, which made the particles collide with the substrate in a less molten state, producing peaks and valleys on the surface of the coating, generating a more irregular surface, and thus increasing the surface roughness.

3.1. Chemical analysis

Table 3 presents the chemical composition of the coating was obtained by EDS from the analysis of a small area of the sample. The EDS is a semi-quantitative method, so this analysis mainly returns to the principal components of the material. To analyze more specific the materials quantity components, other techniques must be used.

Table 3. Chemical composition of the coating.

Elements (%Weight)	Silicon	Chromium	Manganese	Boron	Iron
Coating	1.02	29.69	5.90	-	68.17

The concentrations of silicon, chromium and iron in the coating were similar to those in the wire (Tab. 1). The presence of boron was not evaluated because it is a light element, that is, with an atomic number equal to 5, and it cannot be identified by EDS, which only detects elements with an atomic number greater than 11 [26,27]. The results obtained by EDS showed that the elements present in the wire were incorporated in the coating and in the same proportions.

The use of compressed air as a propulsion gas proved to be reliable for the incorporation of the elements present in the wire, although studies indicate that the use of argon as a propulsion gas is better, since it generates an inert arc and consequently coatings free of oxides and other contaminants [28-30].

3.2. Modeling the heat exchange yield

The heat transfer model presented a flow of 1,252.91 Watts / meter of tube, considering as substrate (uncoated) steel tubes typically used in boilers of thermoelectric plants.

The coating showed a thermal diffusivity of $2.42 \pm 0.39 \text{ mm}^2/\text{s}$ and its presence caused the heat flux to be 1,244.93 Watts / meter of coated tube.

The results obtained through the mathematical model developed showed that the coating presence represented 0.64% of losses for heat transfer in the system. According to Armstrong, one should consider the use of coatings in boiler tubes causes reduce in thermal efficiency of less than 1% [31].

3.3. Microhardness

Figure 4 shows one of the Vickers microhardness (HV) measurement grids made on the coating. The same procedure was performed to determine the microhardness of the substrate and the region of interface between substrate / coating.

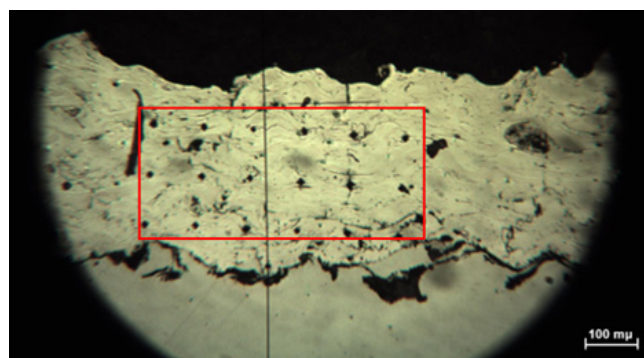


Figure 4. Grid of microhardness measurements in the coating.

Table 4 presents the results for each region analyzed.

Table 4. Vickers microhardness values (HV).

	Average (HV)
Coating	730.54 ± 164.28
Interface Substrate/Coating	21.79 ± 28.27
Substrate	179.26 ± 6.72

The coating microhardness was approximately 3 times higher than that of the substrate and 11% lower than the hardness of coal ash used in a Brazilian thermoelectric power plant, which is 825 HV [32]. The high hardness of coatings is a contributing factor to the longevity of the pipeline. The greater dispersion of measurements for the coating can be attributed to the presence of oxides, cracks and pores [33,34]. The adhesion tests performed according to ASTM C633, showed an average bond strength of 12.06 ± 2.5 MPa [16]. The value is in accordance with that determined by the Petrobras standard N-2568 [35] applied to the Brazilian oil industry and which sets minimum requirements for depositing coatings by TS electric arc applied to tubes and metallic equipment, among which must have a minimum adhesion of 10 MPa.

The Electric Power Research Institute – EPRI establishes that for wire arc thermally sprayed coatings with chemical composition Fe-27Cr-3B-1.5Mn-Si adhesion strength is 40 MPa, but this result will depend on the spray parameters used, the coating surface roughness, the type of adhesive used and its curing time and the adhesion test standard considered [36].

The factors that affect the adhesion strength of the coating are mainly determined by the interfacial phenomena between the coating and the substrate and the microstructure formed, in addition to the residual stresses in the coating. Typically, a coating with a high value of residual stresses will have a lower average adhesion value compared to another coating that does not have high values of residual stress. At elevated temperature levels during deposition, diffusion occurs at the substrate/coating interface layer, which results in mixing of the materials. Depending on the type of interface formed, strong metallurgical bonding can occur, resulting in high values of adhesive strength. Considering TS methods, the substrate surface is generally rough, and the coatings are sprayed at a lower temperature, which reduces atomic diffusion at the substrate/coating interface, generally resulting in lower adhesion. However, greater adhesion forces can be obtained by adjusting the spray parameters and the propulsion gas [36,37].

The percentage of exposed coating area, that is, the fraction of tested area in which the fracture occurred within the coating, presented an average value of $37.91 \pm 19.80\%$. Regarding adhesion tests, the greater the coating area exposed in the test, the greater the adhesion strength and the greater the protection of the coated part in terms of its resistance. The larger the substrate area exposed after the pull-off test, the lower the protection [38].

Figure 5 shows an aspect of the coating surface region after the pull-off test.

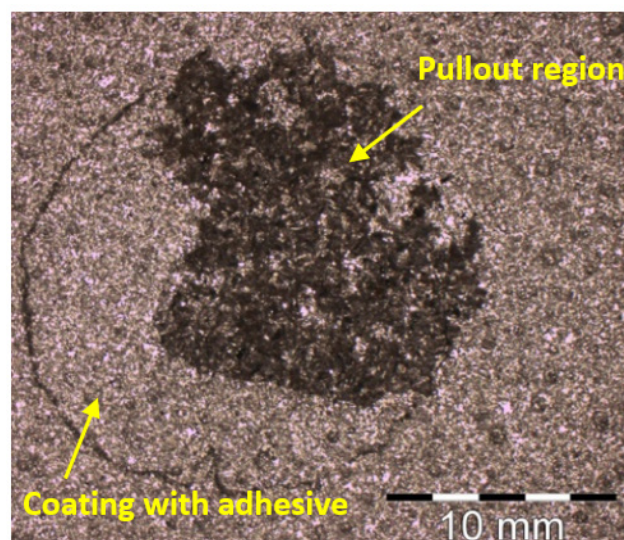


Figure 5. Circular region where the spool was glued in the pull-off test.

The brightest region of the tested area belonged to the region covered with adhesive and the region with the darkest shade belonged to the exposed coating.

EDS performed in the sample area of Figure 5 showed that the brightest regions had energy peaks characteristic of the coating elements and carbon (belonging to the adhesive). Regions of lower brightness (darker hue) showed the significant presence of the elements present in the coating (essentially iron and chromium). The presence of aluminium in this region was attributed to the alumina blasting of the spools. Figure 6a presents a map of false colours assigned to the elements identified over the area of darker shade of Figure 5. Figure 6b presents the spectrum of characteristic energies for the area of Figure 6a.

The results showed that failures of a cohesive nature occurred, that is, the pull-out occurred essentially in the coating and not in the substrate [39]. This fact can be considered promising for the protection activity to be performed by the coating, since the exposure of the substrate is not desired.

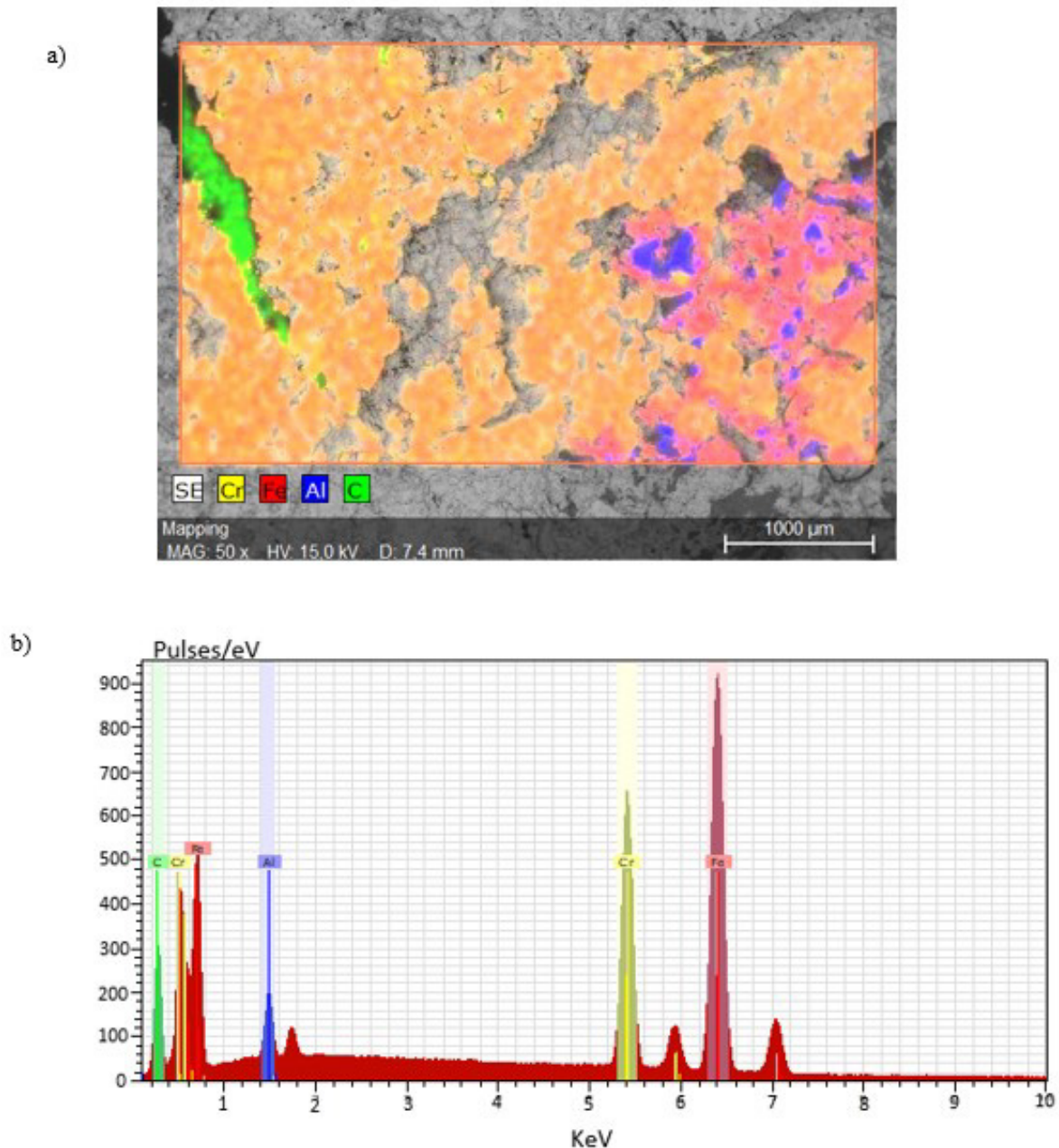


Figure 6. (a) Pull-out surface in the region of darker shade of the spool of **Figure 5** with the identification of the significant presence of the coating elements (iron and chromium); (b) Spectrum of characteristic energies associated with the mapping of the region of (a).

Figure 7 shows the trend of variation between exposed areas of pullout or fracture within the coated layer with measured adhesion stress.

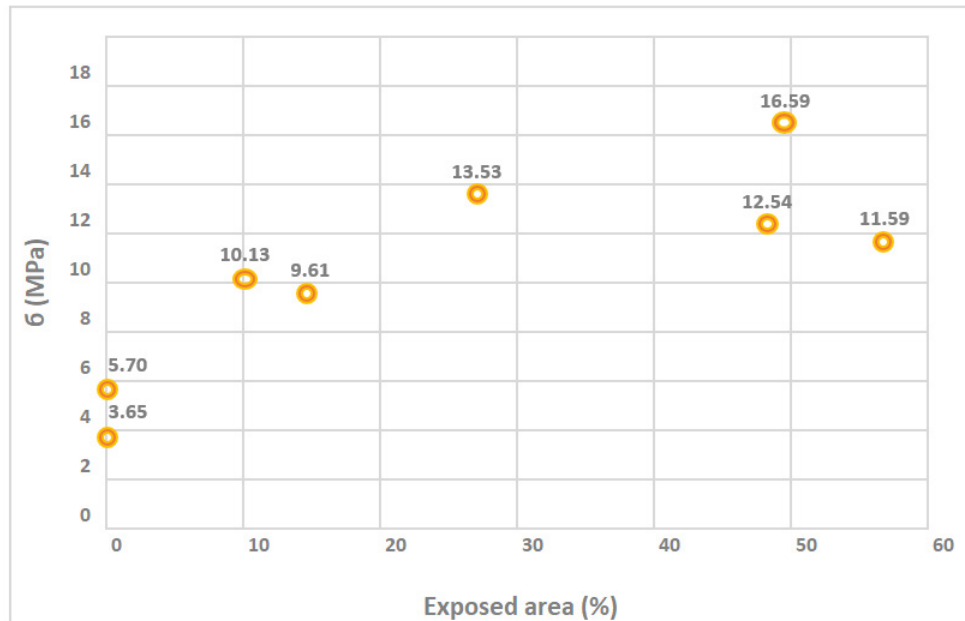


Figure 7. Variation of adhesion tension with the percentage of exposed areas in the adhesion test.

According to Cossenza [23] the precise value of the tension for the test would be determined in the case of total rupture of cohesive nature of the coating, that is, the correct rupture tension for the test would be the one where 100% of rupture of the coating occurred, which it did not occur, although the adhesive used had an average tension of 25 ± 4.1 MPa [23], a value above the maximum obtained in the tests performed with the samples for the present study.

3.4. X-Ray Diffraction

Figure 8 presents the diffractograms obtained for the coating and the substrate.

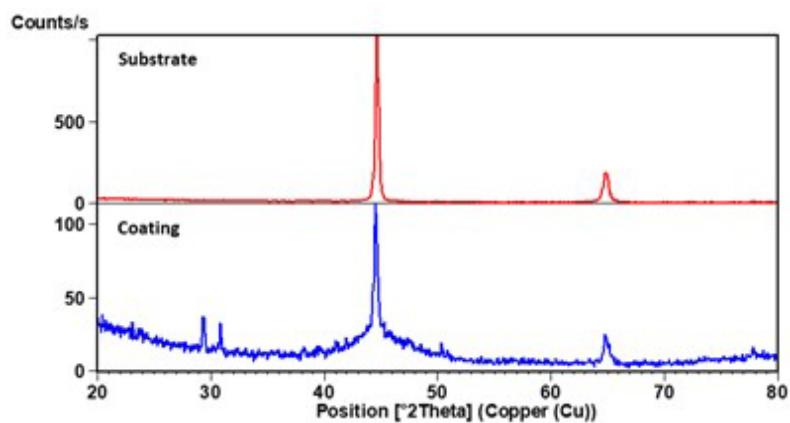


Figure 8. XRD diffractograms of the substrate (above) and the coating.

The results obtained by XRD corroborate the results obtained by EDS, confirming that it is a coating mainly made of Fe-Cr-Si. In the coating diffractogram, the appearance of crystallographic planes referring to the substrate (angles 44° - 46° and 64° - 66°) and diffraction planes at 29 - 31° , 50 - 51° , and 77 - 79° , indicating crystalline phases with characteristic orthorhombic and hexagonal. This way, it be concluded that the process could not amorphized the deposited coating. Although coating amorphization is generally a consequence of the electric arc TS process for iron-based alloys [40-42] and that amorphous coatings are considered more suitable due to their high mechanical strength, high hardness, large elastic deformation limits, hydrophobicity, magnetic properties, good corrosion and wear resistance and thermal stability [43,44], the literature shows that coating metals with crystalline phases have already obtained good durability in service [45-47].

4. Conclusion

The technique and parameters of TS by ASP used promoted the obtaining of a metallic coating with the same chemical composition of the wires originally used, that is, the chemical elements present were incorporated in the coating and in the same proportions. This transfer stability of the wire components to the coating counts positively for the manufacturing process of the coating chosen to be carried out in the field.

The proposed coating presented typical characteristics of metallic coatings sprayed by an electric arc, such as pores and cracks. It was observed that it was deposited homogeneously on the substrate and with an average roughness (R_a) of $247.84 \pm 63.46 \mu\text{m}$. This characteristic is associated with the spray parameters used and affect its wear resistance.

In the mathematical model developed to evaluate the impact of the presence of the coating on the heat transfer in the boiler tube, it implied a reduction of the heat exchange of approximately 0.64%, a value considered within the acceptable range.

The average hardness for the proposed coating was $730.54 \pm 164.28 \text{ HV}$, only 11% lower than the erosive agent (ash) present in boilers powered by pulverized coal in Brazil (825 HV).

The average adhesion strength of the coating was $12.06 \pm 2.5 \text{ MPa}$ and with failures of a cohesive nature without exposure of the substrate, a result considered promising in terms of protecting the substrate when in service.

The XRD test confirmed that even after the electric arc TS procedure, the coating maintained its crystalline characteristic, although iron-based alloys tend to amorphized.

Authors' contribution

PKC: conceptualization, data curation, formal analysis, investigation, methodology, project administration, writing – original draft. BRC, HCF, VSR and ARP: formal analysis, writing – original draft.

MGD: funding acquisition, project administration, supervision, formal analysis, writing – original draft.

Acknowledgements

This study was financed in party by the Coordenação de Aperfeiçoamento de Pessoal de Nível Superior – Brasil (CAPES) – Finance Code 001. The authors wish to thanks the CEPEL - Centro de Pesquisas de Energia Elétrica and IMA – UFRJ - Instituto de Macromoléculas Professora Eloisa Mano da Universidade Federal do Rio de Janeiro.

References

- [1] Veselov FV, Khorshev AA, Erokhina IV, Alikin RO. Economic challenges for coal-fired power plants in russia and around the world. *Power Technology and Engineering*. 2019;53(3):324-330. <http://dx.doi.org/10.1007/s10749-019-01079-9>.
- [2] Zierold KM, Odoh C. A review on fly ash from coal-fired power plants: chemical composition, regulations, and health evidence. *Reviews on Environmental Health*. 2020;35(4):401-418. <http://dx.doi.org/10.1515/reveh-2019-0039>. PMID:32324165.
- [3] Gomes DL. Caracterização de cinzas leves e de revestimento para caldeiras de central termelétrica brasileira [dissertação de mestrado]. Rio de Janeiro: Universidade do Estado do Rio de Janeiro; 2018.
- [4] Alekhnovich AA, Artem'eva NV. Effect of the ash content on the slagging properties of coals and the slagging of pulverized coal-fired boilers. *Power Technology and Engineering*. 2017;51(4):431-437. <http://dx.doi.org/10.1007/s10749-017-0851-7>.
- [5] Srinivasan P, Kushwaha S. Creep life prediction of super heater coils used in coal based thermal power plants subjected to fly ash erosion and oxide scale formation. *IOP Conference Series. Materials Science and Engineering*. 2018;346(1):012008. <http://dx.doi.org/10.1088/1757-899X/346/1/012008>.
- [6] Prashar G, Vasudev H, Thakur L. A case study on the failure analysis, prevention, and control of boiler tubes at elevated temperatures. In Thakur L, Vasudev H, editors. *Thermal spray coatings*. Boca Raton: CRC Press; 2021. p. 347-352. <http://dx.doi.org/10.1201/9781003213185-15>.
- [7] Dhand D, Kumar P, Grewal JS. A review of thermal spray coatings for protection of steels from degradation in coal fired power plants. *Corrosion Reviews*. 2021;39(3):243-268. <http://dx.doi.org/10.1515/correv-2020-0043>.
- [8] Yury K, Filippov M, Makarov A, Malygina I, Soboleva N, Fantozzi D, et al. Arc-sprayed Fe-based coatings from cored wires for wear and corrosion protection in power engineering. *Coatings*. 2018;8(2):71. <http://dx.doi.org/10.3390/coatings8020071>.
- [9] American Society for Testing and Materials. ASTM A-178: standard specification for electric-resistance-welded carbon steel and carbon-manganese steel boiler and superheater tubes. West Conshohocken: ASTM; 2012.
- [10] International Organization for Standardization. ISO 8501-1: preparation of steel substrates before application of paints and related products — Visual assessment of surface cleanliness — Part 1: Rust grades and preparation grades of uncoated steel substrates and of steel substrates after overall removal of previous coatings. Geneva: ISO; 2007.

- [11] Associação Brasileira de Normas Técnicas. ABNT NBR NM ISO 6507-1: materiais metálicos – ensaio de dureza vickers. Parte 1: Método de Ensaio. São Paulo: ABNT; 2008.
- [12] American Society for Testing and Materials. ASTM E1461-13: standard test method for thermal diffusivity by the flash method. West Conshohocken: ASTM; 2013.
- [13] Wu H, Beni MH, Moradi I, Karimipour A, Kalbasi R, Rostami S. Heat transfer analysis of energy and exergy improvement in water-tube boiler in steam generation process. *Journal of Thermal Analysis and Calorimetry*. 2020;139(4):2791-2799. <http://dx.doi.org/10.1007/s10973-019-09034-6>.
- [14] Li L, Li N, Wen D, Yao Y, Zhou Q, Ao Y. Experimental study on heat transfer process in boilers to predict thermal strain/stress distribution and deformation risk of membrane walls. *Process Safety and Environmental Protection*. 2020;138:186-198. <http://dx.doi.org/10.1016/j.psep.2020.03.018>.
- [15] Bergman TL, Lavine AS. *Incropera: fundamentos da transferência de calor e de massa*. 8. ed. Barueri: LTC; 2019.
- [16] American Society for Testing and Materials. ASTM C-633: standard test method for adhesion or cohesion strength of thermal spray coatings. West Conshohocken: ASTM; 2001.
- [17] Lacerda FGB, Braga AVC, Brito TC, Senna LF, Cardoso BR, Furtado HC. Avaliação de defeitos em revestimentos metálicos aspergidos termicamente por arco elétrico em substratos de geometrias distintas. *Brazilian Journal of Development*. 2021;7(2):18891-18904. <http://dx.doi.org/10.34117/bjdv7n2-503>.
- [18] Vaz RF, Sucharski GB, Chicoski A, Siqueira IB, Tristante R, Pukasiewicz AG. Comparison of FeMnCrSi cavitation resistance coatings deposited by twin-wire electric arc and high-velocity oxy-fuel processes. *Journal of Thermal Spray Technology*. 2021;30(3):754-771. <http://dx.doi.org/10.1007/s11666-020-01145-z>.
- [19] Šulcová P, Houdková Š, Duliškovič J. The mechanical properties of coatings sprayed by electric arc for use in coal power plants. *IOP Conference Series. Materials Science and Engineering*. 2021;1178(1):012054. <http://dx.doi.org/10.1088/1757-899X/1178/1/012054>.
- [20] Zhang J, Saha DC, Jahed H. Microstructure and mechanical properties of plasma transferred wire arc spray coating on aluminum cylinder bores. *Surface and Coatings Technology*. 2021;426:127757. <http://dx.doi.org/10.1016/j.surfcoat.2021.127757>.
- [21] Azarmi F, Sevostianov I. Comparative micromechanical analysis of alloy 625 coatings deposited by air plasma spraying, wire arc spraying, and cold spraying technologies. *Mechanics of Materials*. 2020;144:103345. <http://dx.doi.org/10.1016/j.mechmat.2020.103345>.
- [22] Arif ZU, Arif ZU, Shah M, Rehman EU, Rehman EU, Tariq A. Effect of spraying parameters on surface roughness, deposition efficiency, and microstructure of electric arc sprayed brass coating. *International Journal of Advanced and Applied Sciences*. 2020;7(7):25-39. <http://dx.doi.org/10.21833/ijaas.2020.07.004>.
- [23] Cossenza MM. Caracterização de revestimento metálico à base de ferro-cromo-nióbio obtido por aspersão térmica para tubos de caldeiras que operam a carvão mineral [dissertação de mestrado]. Rio de Janeiro: Universidade do Estado do Rio de Janeiro; 2018.
- [24] Belém MJX, Lima, CRC, Kuhl A, Camargo F. (2020). Avaliação da resistência ao desgaste erosivo e abrasivo de revestimentos WC 12Co aplicados por aspersão térmica HVOF. *Revista Matéria*. 25(1):1-13. <http://dx.doi.org/10.1590/S1517-707620200001.0909>.
- [25] Khakpour A, Uhrlandt D, Methling RP, Gortschakow S, Franke S, Imani MT, et al. Impact of temperature changing on voltage and power of an electric arc. *Electric Power Systems Research*. 2017;143:73-83. <http://dx.doi.org/10.1016/j.epr.2016.10.009>.
- [26] Nasrazadani S, Hassani S. Modern analytical techniques in failure analysis of aerospace, chemical, and oil and gas industries. In: Makhlof ASH, Aliofkhaezrai M, editors. *Handbook of materials failure analysis with case studies from the oil and gas industry*. Reino Unido: Butterworth-Heinemann; 2016. Cap. 2, p. 39-54. <https://doi.org/10.1016/B978-0-08-100117-2.00010-8>.
- [27] Swapp S. *Scanning Electron Microscopy (SEM)*. Canada: Science Education Resource Center Carleton College; 2017 [access 11 october 2021]. Available from https://serc.carleton.edu/research_education/geochemsheets/techniques/SEM.html
- [28] Fiebig J, Bakan E, Kalfhaus T, Mauer G, Guillon O, Vaßen R. Thermal spray processes for the repair of gas turbine components. *Advanced Engineering Materials*. 2020;22(6):1901237. <http://dx.doi.org/10.1002/adem.201901237>.
- [29] Erfanmanesh M, Reza Bakhshi S, Khajelakzay M, Salekbafighi M. The effect of argon shielding gas at plasma spray process on the structure and properties of MoSi₂ coating. *Ceramics International*. 2014;40(3):4529-4533. <http://dx.doi.org/10.1016/j.ceramint.2013.08.128>.
- [30] Shankar S, Koenig DE, Dardi LE. Vacuum plasma sprayed. Vacuum plasma sprayed metallic coatings. *JOM*. 1981;33(10):13-20. <http://dx.doi.org/10.1007/BF03339507>.
- [31] Armstrong M, Sivasubramanian M, Selva Palam N, Adam Khan M, Rajaganapathy C. A recent examination on the nano coating techniques in heat transfer applications. *Materials Today: Proceedings*, 2021;46(Pt 17):7942-7. <http://dx.doi.org/10.1016/j.matpr.2021.02.660>.
- [32] Gomes DL, Cardoso BR, Furtado HC, Diniz MG. Characterization of fly ash and a protective coating for brazilian thermal power plant boilers. *Materials Research*. 2020;23(6):e20200257. <http://dx.doi.org/10.1590/1980-5373-mr-2020-0257>.

- [33] Swain B, Mallick P, Gupta RK, Mohapatra SS, Yasin G, Nguyen TA, et al. Mechanical and tribological properties evaluation of plasma-sprayed shape memory alloy coating. *Journal of Alloys and Compounds*. 2021;863:158599. <http://dx.doi.org/10.1016/j.jallcom.2021.158599>.
- [34] Wagner N. Effect of process parameters on twin wire arc sprayed steel coatings. *Journal of Materials Engineering and Performance*. 2021;30(9):6650-6655. <http://dx.doi.org/10.1007/s11665-021-05941-8>.
- [35] Petrobrás. PETROBRÁS N-2568: Revestimentos metálicos por aspersão térmica. Rio de Janeiro: EPRI; 2011.
- [36] Electric Power Research Institute. State of knowledge review of nanostructured coatings for boiler tube applications.. 2007. Technical Update.
- [37] Eden T, Wolfe D. (2007). Cold spray particle deposition for improved wear resistance. In: Champagne VK, editor. *The cold spray materials deposition process: fundamentals and applications*. USA: Elsevier. p. 264-301. <http://dx.doi.org/10.1533/9781845693787.3.264>.
- [38] Pathanatecha W. A study of various parameters affecting adhesion of coatings to metal substrates. Degree project in chemical science and engineering second level, 30 credits. Sweden: Mårsta; 2019.
- [39] American Society for Testing and Materials. ASTM D 4541-02: standard test method for pull-off strength of coatings using portable adhesion tester. West Conshohocken: ASTM; 2002.
- [40] Wang Q, Han P, Yin S, Niu W-J, Zhai L, Li X, et al. Current research status on cold sprayed amorphous alloy coatings: a review. *Coatings*. 2021;11(2):206. <http://dx.doi.org/10.3390/coatings11020206>.
- [41] Zhang H, Gong Y, Chen X, McDonald A, Li H. A comparative study of cavitation erosion resistance of several HVOF-sprayed coatings in deionized water and artificial seawater. *Journal of Thermal Spray Technology*. 2019;28(5):1060-1071. <http://dx.doi.org/10.1007/s11666-019-00869-x>.
- [42] Luo J, Shi N, Xing Y, Jiang C, Chen Y. (2019). Effect of arc power on the wear and high-temperature oxidation resistances of plasma-sprayed Fe-based amorphous coatings. *High Temperature Materials and Processes*. 38(2019):639-646. <http://dx.doi.org/10.1515/htmp-2019-0003>.
- [43] Iqbal A, Siddique S, Maqsood M, Atiq Ur Rehman M, Yasir M. Comparative analysis on the structure and properties of iron-based amorphous coating sprayed with the thermal spraying techniques. *Coatings*. 2020;10(10):1006. <http://dx.doi.org/10.3390/coatings10101006>.
- [44] Lin JR, Wang ZH, Lin PH, Cheng JB, Zhang X, Hong S. Effect of crystallisation on electrochemical properties of arc sprayed FeNiCrBSiNbW coatings. *Surface Engineering*. 2014;30(9):683-687. <http://dx.doi.org/10.1179/1743294414Y.0000000299>.
- [45] Sharma RK, Das RK, Kumar SR. Effect of chromium content on microstructure, mechanical and erosion properties of Fe-Cr-Ti-Mo-C-Si coating. *Surfaces and Interfaces*. 2021;22:100820. <http://dx.doi.org/10.1016/j.surfin.2020.100820>.
- [46] Duarte MJ, Kostka A, Jimenez JA, Choi P, Klemm J, Crespo D, et al. (2014). Rystallization, phase evolution and corrosion of Fe-based metallic glasses: an atomic-scale structural and chemical characterization study. *Acta Materialia*. 71:20-30. <https://doi.org/10.1016/j.actamat.2014.02.027>.
- [47] Kant S, Kumar M, Chawla V, Singh S. Study of high temperature oxidation behavior of wire arc sprayed coatings. *Materials Today: Proceedings*. 2020;21:1741-1748.